Hydrol. Earth Syst. Sci. Discuss., doi:10.5194/hess-2016-282, 2016
Manuscript under review for journal Hydrol. Earth Syst. Sci.
Published: 23 June 2016

Hydrology and Earth System Sciences
Open Access
Discussions

Evaluating the streamflow simulation capability of PERSIANN-CDR daily rainfall products in two river basins on the Tibetan Plateau

Xiaomang Liu[1,2], Tiantian Yang[2], Koulin Hsu[2], Changming Liu[1] and Soroosh Sorooshian[2]

1 Key Laboratory of Water Cycle & Related Land Surface Process, Institute of Geographic Sciences and Natural Resources Research, Chinese Academy of Sciences, 100101 Beijing, China
2 Department of Civil and Environmental Engineering, University of California, Irvine, California, USA

*Corresponding author: Tiantian Yang, Email: tiantiay@uci.edu

Hydrol. Earth Syst. Sci. Discuss., doi:10.5194/hess-2016-282, 2016
Manuscript under review for journal Hydrol. Earth Syst. Sci.
Published: 23 June 2016

Hydrology and Earth System Sciences
Open Access
Discussions

Abstract:

On the Tibetan Plateau, the limited ground-based rainfall information owing to a harsh environment has brought great challenges to hydrological studies. Satellite-based rainfall products, which allow a better coverage than both radar network and rain gauges on the Tibetan Plateau, can be suitable observation alternatives for investigating the hydrological processes and climate change. In this study, a newly developed daily satellite-based precipitation product, termed Precipitation Estimation from Remotely Sensed Information Using Artificial Neural Networks–Climate Data Record (PERSIANN-CDR), is used as input of a hydrologic model to simulate streamflow in the upper Yellow and Yangtze River Basin on the Tibetan Plateau. The results show that the simulated streamflow using PERSIANN-CDR precipitation is closer to observation than that using limited gauge-based precipitation interpolation in the upper Yangtze River Basin. The simulated streamflow using gauge-based precipitation are higher than the streamflow observation during the wet season. In the upper Yellow River Basin, PERSIANN-CDR precipitation and gauge-based precipitation have similar good performance in simulating streamflow. The evaluation of streamflow simulation capability in this study partly indicates that PERSIANN-CDR rainfall product has good potentials to be a reliable dataset and an alternative information source besides the sparse gauge network for conducting long term hydrological and climate studies on the Tibetan Plateau.

Key Words: PERSIANN-CDR daily rainfall product; Streamflow simulation; Tibetan Plateau

1. Introduction

Precipitation is one of the essential meteorological inputs of hydrologic model and the key driving force for hydrologic cycle. Errors in precipitation estimation can bring significant uncertainties in streamflow simulation and prediction (Sorooshian et al., 2011). Three methods are

Hydrol. Earth Syst. Sci. Discuss., doi:10.5194/hess-2016-282, 2016
Manuscript under review for journal Hydrol. Earth Syst. Sci.
Published: 23 June 2016

generally used to measure precipitation: traditional gauge observations, meteorological radar observations and satellite observations (Ashouri et al., 2015). In many remote regions and mountainous area, rain gauges and meteorological radar networks are either sparse or non-existent. Thus, satellite-based precipitation is of great importance in such regions. For instance, there is a great potential of using satellite-based precipitation estimate on the Tibetan Plateau known as the "roof of the world" with an average elevation of over 4000m (Yao et al., 2012). Owing to a harsh environment, the existing meteorological stations managed by the Chinese Meteorological Administration only form an extremely sparse network, which create great challenges for water resources management and operation. For example, on average, there is only 0.3 and 1 station per grid of 1°×1° in the upper Yangtze and upper Yellow river basins, respectively. Moreover, the spatial distribution of the meteorological stations is highly uneven and most stations are located around the river channel with relatively low elevation [Figure 1]. Therefore, streamflow simulation using the limited gauge-based rainfall information might not be reliable due to the input uncertainties with such a poor spatial resolution. Satellite-based rainfall products have the advantage of good spatial coverage, which could allow an accurate streamflow simulation on the Tibetan Plateau.

According to Kidd and Levizzani (2011), during the last decade satellite-based precipitation estimates have reached a good level of maturity. Currently, there are many satellite rainfall products are available and have been extensively used globally (e.g., Sorooshian et al., 2000; Huffman et al., 2001; Adler et al., 2003; Xie et al., 2003; Joyce et al., 2004; Turk and Miller, 2005). Recently, a new satellite-based precipitation product is released by National Climatic Data Center (NCDC), which is termed Precipitation Estimation from Remotely Sensed Information Using Artificial Neural Networks–Climate Data Record (PERSIANN-CDR) (Ashouri et al., 2015).

Hydrol. Earth Syst. Sci. Discuss., doi:10.5194/hess-2016-282, 2016
Manuscript under review for journal Hydrol. Earth Syst. Sci.
Published: 23 June 2016

PERSIANN-CDR is a multi-satellite, high-resolution and post-time rainfall product that provides daily precipitation estimates at 0.25˚ spatial resolution from 1 January 1983 to the present. According to Ashouri et al., (2015), PERSIANN-CDR rainfall product uses the archive of Gridded Satellite (GridSat-B1) Infrared Radiation (IR) data (Knapp, 2008) as the input to the Artificial Neural Network algorithm. The retrieval algorithm uses IR satellite data from global geosynchronous satellites as the primary source of precipitation information. To meet the calibration requirement of PERSIANN, the model is pre-trained using the National Centers for Environmental Prediction (NCEP) stage IV hourly precipitation data. Then, the parameters of the model are kept fixed and the model is run for the full historical record of GridSat-B1 IR data. To reduce the biases in the estimated precipitation, while preserving the temporal and spatial patterns in high resolution, the resulting estimates are then adjusted using the Global Precipitation Climatology Project (GPCP) monthly 2.5˚ precipitation products. The performance of PERSIANN-CDR rainfall product has been tested and reported in different regions (Ashouri et al. 2015; Casse et al. 2015; Miao et al., 2015). Ashouri et al. (2015) found that PERSIANN-CDR precipitation is performing reasonably well when compared with radar and ground-based observations in the 1986 Sydney flood event of Australia and the 2005 Hurricane Katrina of United States. Miao et al. (2015) shows that PERSIANN-CDR rainfall product is able to capture the spatial and temporal characteristics of extreme precipitation events at daily scale in the eastern China monsoon region when compared with ground-based precipitation dataset. Casse et al. (2015) employed PERSIANN-CDR to simulate the flood events in Niamey River and compared with multiple datasets. It was found out by Casse et al. (2015) that the simulated streamflow with PERSIANN-CDR has high correlation as compared to streamflow observation. Miao et al. (2015) also pointed out that the correlation between the PERSIANN-CDR precipitation and ground-based

Hydrol. Earth Syst. Sci. Discuss., doi:10.5194/hess-2016-282, 2016
Manuscript under review for journal Hydrol. Earth Syst. Sci.
Published: 23 June 2016

93 precipitation is not strong on the Tibetan Plateau and speculated that the sparse ground-based
94 gauge stations may result in uncertainties of the use of ground-based precipitation estimates as
95 reference on the Tibetan Plateau. Building on Miao et al. (2015), in this study, PERSIANN-CDR
96 is further applied to a conceptual hydrological model to simulate streamflow of two river basins
97 on the Tibetan Plateau. The simulated streamflow with PERSIANN-CDR is compared with that
98 forced by limited gauge information, as well as the streamflow observations at the outlets of these
99 two basins.

100 Many studies have been carried out to evaluate the suitability of a number of satellite-based
101 precipitation estimate products in forcing hydrologic models and simulating streamflow for
102 various regions around the world (e.g., Yilmaz et al., 2005; Artan et al., 2007; Su et al., 2011; Bitew
103 et al., 2012; Yong et al., 2012). However, there are few evaluation works focusing on hydrological
104 modeling driven by satellite rainfall products on the Tibetan Plateau. Among limited number of
105 studies, Tong et al. (2014) evaluated the streamflow simulation capability of four satellite products
106 (TRMM-3B42-V7, TRMM-3B42RT-V7, PERSIANN and CMORPH) using the Variable
107 Infiltration Capacity (VIC) hydrologic model in two sub-basins over the Tibetan Plateau and
108 concluded that the TRMM-3B42-V7 and CMORPH datasets have relative better performance than
109 others. One of the limitations is that the data of many satellite precipitation products, such as
110 TRMM-3B42RT-V7 and CMORPH only starts from 2000 to the present, which is rather short. In
111 this study, there is no such limitation because PERSIANN-CDR daily rainfall product includes
112 more than 33 years of data and the length of data grows every year. In Tong et al, (2014), the rain-
113 gauge is set to be reference to compare different satellite-based rainfall products. However, given
114 the facts that (1) density of rain-gauges on Tibetan Plateau is rather low as compared to other
115 regions in China, (2) distribution of gauges are uneven according to the investigation from Miao

Hydrol. Earth Syst. Sci. Discuss., doi:10.5194/hess-2016-282, 2016
Manuscript under review for journal Hydrol. Earth Syst. Sci.
Published: 23 June 2016

et al, (2015), and (3) rain-gauges are located in low elevation river channels (Figure 1), authors have the similar concern as Miao et al, (2015) that the use of sparse rain-gauge network as reference to compare satellite products is questionable. Therefore, in this study, both PERSIANN-CDR daily rainfall product and ground-based rainfall information are used as the inputs of a hydrologic model for streamflow simulation on two major river basins, the upper Yangtze River Basin and the upper Yellow River Basin, on the Tibetan Plateau. Then, the simulation results are compared with observed streamflow, which is believed to be a more reliable reference than the limited rainfall observation to judge the qualities of satellite rainfall products on the Tibetan Plateau. The uncertainty sources are also discussed with regard to the parameterization of hydrological model and the length of data used for calibration.

2. Study region, data and hydrological modeling

2.1 Study region and data

Two river basins on the northern Tibetan Plateau, namely, the upper Yangtze River (UYZR) and upper Yellow River (UYLR) basins are selected, which have a long daily streamflow record from 1983 to 2012. As shown with red squares in Figure 1, two hydrological stations, Tangnaihai and Zhimenda, are the outlet stations of the UYZR and UYLR, which have total drainage areas of 121,972 and 137,704 km^2, respectively. Elevation in the region varies from 3450 to 6621 m. According to Yao et al. (2012), the climate system of the two selected regions have distinct summer Indian monsoon and East Asian monsoon characteristics during summer. Figure 1 shows the distribution of meteorological and hydrological stations in the two basins. The green triangles show the locations of rain-gauges, which are rather unevenly distributed and sparse as compared to the gauge distribution of in other regions of China (Miao et al., 2015).

Hydrol. Earth Syst. Sci. Discuss., doi:10.5194/hess-2016-282, 2016
Manuscript under review for journal Hydrol. Earth Syst. Sci.
Published: 23 June 2016

Hydrology and Earth System Sciences
Discussions

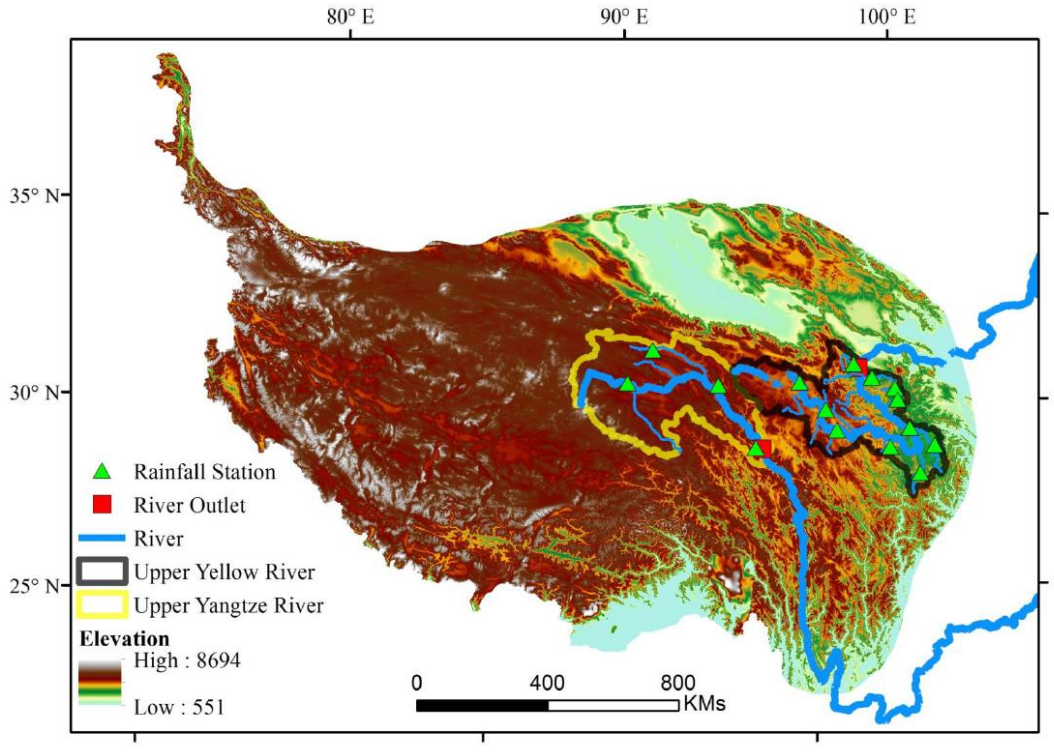

139

140 Figure 1. The selected river basins (the upper Yellow River and Yangtze River Basin) on the
141 Tibetan Plateau and location of rainfall stations and river outlets.

142

143 The observed daily streamflow data from 1983 to 2012 at the outlets of the two basins is provided
144 by the Ministry of Water Resources of China. The runoff is calculated by dividing streamflow by
145 corresponding basin area. The daily gauge meteorological data in the two basins from 1983 to
146 2012 is obtained from the China Meteorological Administration (http://cdc.cma.gov.cn). There are
147 4 and 11 meteorological stations in the UYZR and UYLR respectively, which means that on
148 average there is only 0.3 and 1 station per grid of 1˚×1˚ in the two basins, respectively. The
149 PERSIANN-CDR rainfall dataset is available at the NOAA NCDC website
150 (ftp://data.ncdc.noaa.gov/cdr/persiann/files/), as well as the Center for Hydrometeorology and

Hydrol. Earth Syst. Sci. Discuss., doi:10.5194/hess-2016-282, 2016
Manuscript under review for journal Hydrol. Earth Syst. Sci.
Published: 23 June 2016

Remote Sensing (CHRS) at the University of California, Irvine. In order to compare PERSIANN-CDR with gauge observation, the gauge precipitation is interpolated into 0.25°×0.25° grids with the inverse distance weighting interpolation method, which has been demonstrated as being efficient in precipitation interpolation applications (e.g., Nalder and Wein, 1998; Garcia et al., 2008; Ly et al., 2011). The daily gauge-based precipitation and PERSIANN-CDR precipitation for basin average are compared by the cumulative distribution functions (CDFs) of daily precipitation value (e.g., Sheffield et al., 2014; Zhang and Tang, 2015), wherein the two-parameter Gamma distribution function (Thom, 1958) is used to fit the data.

2.2 Hydrological modeling

The hydrologic model used in this study is the Hydro-Informatic Modeling System (HIMS) rainfall-runoff model (Liu et al., 2006, 2008, 2010a, 2010b), which is one of the operational hydrological models in practice by the Tibet Government in China. The HIMS model is a grid-based hydrologic model, which is able to simulate the dominant hydrological processes such as actual evapotranspiration, infiltration, runoff, groundwater recharge and channel routing. In HIMS model, a catchment is divided into grids, and grids are linked throughout the stream network based on topological relationships of channel network and properties of soil, vegetation and land use. In each grid, actual evaporation is calculated by a formulation between soil water content and potential evapotranspiration. Potential evapotranspiration ET_0 (Hargreaves and Samani, 1985) and actual evaporation ET_a are described as follows:

$$ET_0 = 0.00023 \cdot RA \cdot (T + 17.8) \cdot (T_{\max} - T_{\min})^{0.50} \quad (1)$$

$$ET_a(t) = ET_0(t) \cdot (1 - (1 - \frac{SMS_t}{SMSC})^C) \quad (2)$$

where RA is extraterrestrial radiation (MJ m^{-2} d^{-1}); T, T_{max} and T_{min} are daily average, maximum and minimum temperatures, respectively (°C); L is latent heat of vaporization (MJ kg^{-1}); SMS and

Hydrol. Earth Syst. Sci. Discuss., doi:10.5194/hess-2016-282, 2016
Manuscript under review for journal Hydrol. Earth Syst. Sci.
Published: 23 June 2016

174 *SMSC* are soil moisture storage and the maximum soil storage capacity (mm), respectively; and *C*
175 is the evapotranspiration coefficient in need of calibration.

176 Infiltration is modeled using an empirical relationship, which has been confirmed through
177 analysis of data measured in a number of experimental watersheds and various physical geographic
178 factors in China (Liu et al., 2006):

179 $$f_t = R \cdot P_t^r \tag{3}$$

180 where f_t is infiltration (mm) and P_t is precipitation (mm). R and r are parameters. Surface runoff
181 RS_t (mm) is calculated by:

182 $$RS_t = P_t - f_t = P_t - R \cdot P_t^r \tag{4}$$

183 According to the saturation excess mechanism and spatial variability of watershed
184 characteristics, interflow and groundwater recharge are estimated as linear functions of soil
185 wetness (soil moisture amount divided by soil moisture capacity). Baseflow is simulated based on
186 the linear reservoir assumption, in which the relationship between groundwater storage and
187 outflow is linear. Interflow *RI* (mm), groundwater recharge *REC* (mm), baseflow *RG* (mm), and
188 total runoff *TR* (mm) are determined by:

189 $$RI_t = L_a \times (SMS_t / SMSC) \times f_t \tag{5}$$

190 $$REC_t = R_C \times (SMS_t / SMSC) \times (f_t - RI_t) \tag{6}$$

191 $$RG_t = K_b \times (GW_t + REC_t) \tag{7}$$

192 $$TR_t = RS_t + RI_t + RG_t \tag{8}$$

193 where L_a, R_c and K_b are efficiencies for interflow, groundwater recharge and baseflow, respectively;
194 *SMSC* is the maximum value of soil moisture storage capacity (mm); *SMS* is actual soil moisture
195 storage (mm); and *GW* is groundwater storage (mm). L_a, R_c, K_b and *SMSC* are parameters in need

Hydrol. Earth Syst. Sci. Discuss., doi:10.5194/hess-2016-282, 2016
Manuscript under review for journal Hydrol. Earth Syst. Sci.
Published: 23 June 2016

196 of calibration. The degree-day snowmelt algorithm (Hock, 2003) assuming an empirical
197 relationship between air temperature and snowmelt rate is used to simulate snowmelt runoff. The
198 air temperature within each grid is adjusted by a commonly used temperature lapse rate
199 (0.65°C/100m). The degree-day factor of snowmelt is set to 4.1 $mm°C^{-1}$ day^{-1} in the two basins
200 based on the investigation of Zhang et al. (2006). Surface runoff and baseflow for each grid are
201 routed to the basin outlet through a channel network. The Muskingum method (Franchini and
202 Lamberti, 1994) is used for flow channel routing. The detail descriptions of HIMS model refer to
203 Liu et al. (2008) and Jiang et al. (2015).

204 The HIMS model is set up at 0.25°×0.25° spatial resolution grids in the two river basins.
205 There are nine parameters requiring calibration in the HIMS model (Table 1). The Shuffle Complex
206 Evolution method (SCE-UA) is used for calibrating the model parameters (Duan et al., 1992). The
207 optimization objective is to maximize the Nash-Sutcliffe efficiency (*NSE*) (Nash and Sutcliffe,
208 1970) between the simulated and measured daily streamflow. There are two stopping criteria for
209 calibrating the parameters. The first one is the evolution of all simplexes have converged to a
210 limited parameter space, which is the default convergence criterion of SCE-UA. Another stopping
211 criterion is the maximum number of function evaluation set by users is met. In our study, the
212 settings for SCE-UA are: maximum number of function evaluation equals to 5×10^{8}; numbers of
213 complexes equals to 2; and the percentage change allowed to define convergence is set to 1×10^{-6}.
214 The calibration period is from 1983 to 1997 and the verification period is from 1998 to 2012. The
215 performance of the streamflow simulation is evaluated by comparing simulated and observed
216 streamflow through two statistics: *NSE* and relative bias (*Rb*) between simulated and observed
217 streamflow:

Hydrol. Earth Syst. Sci. Discuss., doi:10.5194/hess-2016-282, 2016
Manuscript under review for journal Hydrol. Earth Syst. Sci.
Published: 23 June 2016

Hydrology and Earth System Sciences
Discussions

$$NSE = 1 - \frac{\sum_{i=1}^{N}(Q_{obs,i} - Q_{sim,i})^2}{\sum_{i=1}^{N}(Q_{obs,i} - \overline{Q_{obs}})^2} \quad (9)$$

$$Rb = \frac{\sum_{i=1}^{N}(Q_{sim,i} - Q_{obs,i})}{\sum_{i=1}^{N} Q_{obs,i}} \quad (10)$$

where Q_{sim} and Q_{obs} are the simulated and observed streamflow, respectively; $\overline{Q_{obs}}$ is the mean of the observed streamflow; and N is the total number of days in the calibration period.

Table 1. Description of HIMS model parameters and allowable ranges.

Parameter	Description	Allowable range
SMSC	The maximum soil storage capacity (mm)	50-1000
R	The infiltration coefficient	0.1-2
r	The infiltration coefficient	0.1-1
L_a	The interflow coefficient	0.1-2
R_C	The groundwater recharge coefficient	0.01-2
C	The evapotranspiration coefficient	0.001-10
K_b	The baseflow coefficient	0.001-1
C_1	The Muskingum coefficient	0.001-1
C_2	The Muskingum coefficient	0.001-1

3. Results

3.1 Hydrometrological characteristics of the two basins

Figure 2 and Table 2 show the average monthly amounts of precipitation and runoff in the UYZR and UYLR from 1983 to 2012. These two river basins have distinct dry and wet seasons, which are from Sep. to Feb., and Mar. to Oct., respectively. According to Table 2, precipitation between May and October (wet season) accounts for 92.5% and 90.1% of the annual total precipitation for the UYZR and UYLR, respectively. . Similar to the temporal distribution of

Hydrol. Earth Syst. Sci. Discuss., doi:10.5194/hess-2016-282, 2016
Manuscript under review for journal Hydrol. Earth Syst. Sci.
Published: 23 June 2016

precipitation, runoff during May to October accounts for 87.6% and 78.4% of annual runoff in the two basins, respectively. Given the seasonal concurrence of precipitation and runoff, thus, precipitation in wet season plays a dominant role in annual runoff generation in these two river basins. The runoff coefficients are 0.22 and 0.26 in the UYZR based on gauge-based precipitation and PERSIANN-CDR precipitation, respectively. In the UYLR, the runoff coefficient is 0.29 based on both gauge-based and PERSIANN-CDR precipitation.

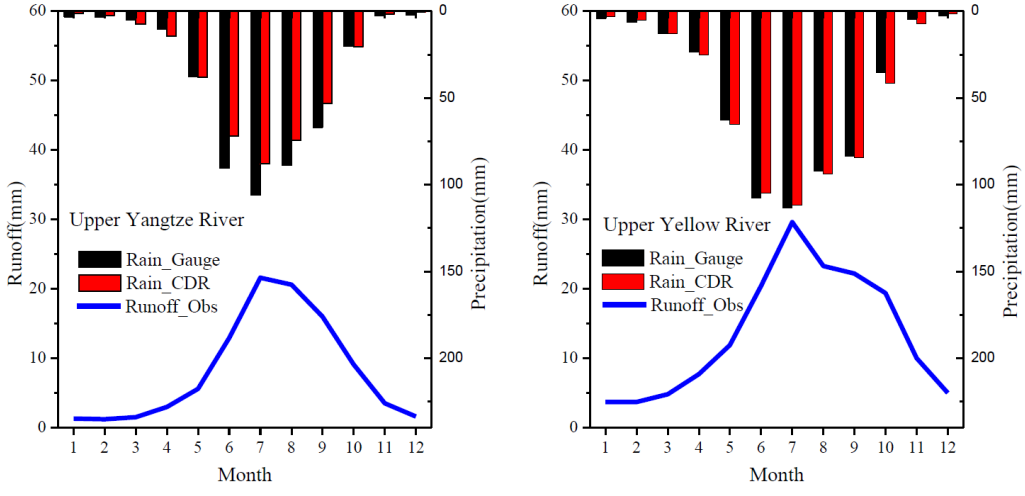

Figure 2. The monthly average runoff observed at the river outlet of the upper Yangtze River and Yellow River Basin, and the precipitation data retrieved from PERSIANN-CDR and ground-based observation.

3.2 Comparison between gauge-based precipitation and PERSIANN-CDR precipitation

Figure 3 shows the comparison of CDFs for basin-averaged daily gauge-based precipitation and PERSIANN-CDR precipitation in the UYZR and UYLR from 1983 to 2012. At a given probability, daily precipitation of PERSIANN-CDR product is generally smaller than gauge-based precipitation in the UYZR. In the UYLR, the CDFs of PERSIANN-CDR precipitation and gauge-

Hydrol. Earth Syst. Sci. Discuss., doi:10.5194/hess-2016-282, 2016
Manuscript under review for journal Hydrol. Earth Syst. Sci.
Published: 23 June 2016

based precipitation show overall better agreement than that in the UYZR. Table 2 shows the average monthly amounts of gauge-based precipitation and PERSIANN-CDR precipitation. Gauge-based precipitation is larger than PERSIANN-CDR precipitation in wet season (Jun., Jul., Aug. and Sep.) in the UYZR, while gauge-based precipitation and PERSIANN-CDR precipitation have similar values in the UYLR. In the UYZR, the average annual precipitation is 436.4 mm from gauge-based data and 374.3 mm from PERSIANN-CDR product, and the former is 16.6% larger than the latter. In the UYLR, average annual amounts of gauge-based precipitation and PERSIANN-CDR precipitation are similar, which are 550.2 and 556.6 mm, respectively (Table 2).

Table 2. Average monthly precipitation and runoff in the upper Yangtze and Yellow River basins

Period	Upper Yangtze River			Upper Yellow River		
	Rain_ Gauge	Rain_ CDR	Runoff_ OBS	Rain_ Gauge	Rain_ CDR	Runoff_ OBS
Jan.	3.3	1.4	1.3	4.4	3.2	3.7
Feb.	3.4	2.5	1.2	6.5	5.2	3.7
Mar.	5.0	7.5	1.5	12.9	13.1	4.8
Apr.	10.2	14.6	3.0	23.7	25.0	7.7
May	37.9	38.2	5.6	62.9	65.3	11.9
Jun.	90.4	72.0	12.9	107.6	104.6	20.4
Jul.	105.8	87.8	21.6	113.5	111.8	29.6
Aug.	88.6	74.5	20.6	92.0	94.0	23.3
Sep.	66.9	53.2	16.0	83.4	84.4	22.2
Oct.	20.2	20.5	9.1	35.3	41.4	19.4
Nov.	2.5	1.7	3.5	5.0	7.3	10.0
Dec.	2.3	0.5	1.6	3.0	1.5	5.0
May to Oct.	409.7	346.1	85.8	494.6	501.4	126.8
Annual	436.4	374.3	98.0	550.2	556.6	161.8
Ratio	93.9	92.5	87.6	89.9	90.1	78.4

Note: Rain_Gauge and Rain_CDR indicate gauge-based precipitation and PERSIANN-CDR precipitation (mm), respectively. Runoff_OBS indicates observed runoff (mm). Ratio means the percentage of precipitation and streamflow during May to November to annual values.

Hydrol. Earth Syst. Sci. Discuss., doi:10.5194/hess-2016-282, 2016
Manuscript under review for journal Hydrol. Earth Syst. Sci.
Published: 23 June 2016

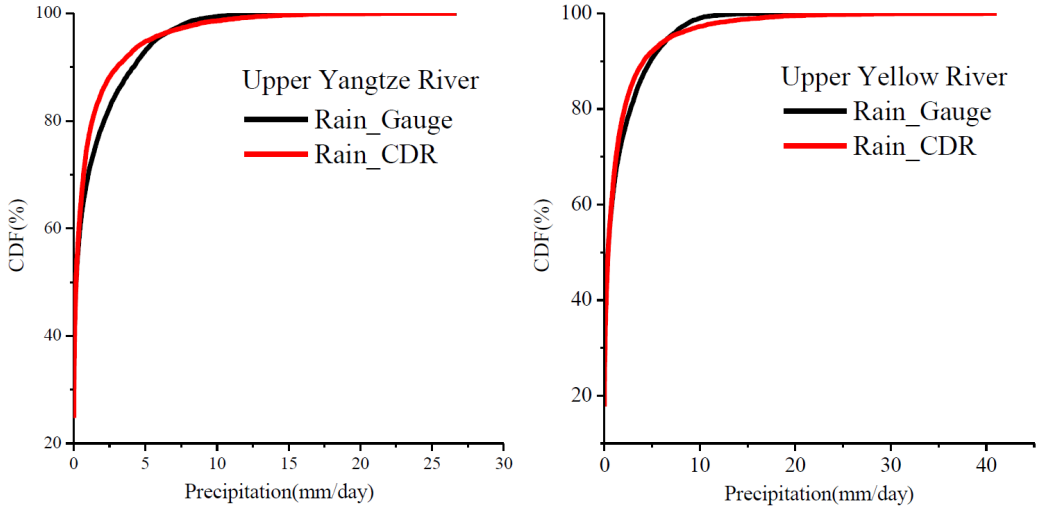

Figure 3. The calculated CDF of rainfall from PERSIANN-CDR and ground-based observation in the upper Yangtze River Basin and upper Yellow River Basin.

3.3 Streamflow Simulation in the two basins

Due to the fact that sparse gauge-network and its interpolation cannot perfectly describe the spatial and temporal rainfall characteristics at river basin scale, the alternative is to evaluate streamflow simulated instead of over-confidently using sparse gauge-network as reference. In this section, the streamflow simulated by both gauge-based precipitation and PERSIANN-CDR precipitation are derived from HIMS model, and compared with observed streamflow at the outlet in the UYZR and UYLR. The HIMS model is separately calibrated by maximizing the *NSE* between observed streamflow and simulated streamflow driven by gauge-based precipitation and PERSIANN-CDR precipitation from 1983 to 1997. Table 3 shows the calibrated parameter values of the HIMS model for the two basins. Figure 4 shows daily observed streamflow and simulated streamflow driven by gauge-based precipitation and PERSIANN-CDR precipitation for the two

Hydrol. Earth Syst. Sci. Discuss., doi:10.5194/hess-2016-282, 2016
Manuscript under review for journal Hydrol. Earth Syst. Sci.
Published: 23 June 2016

278 basins from 1983 to 2012. In the UYLR (Figure 4 (a) and (b)), the *NSE* values between daily
279 observed streamflow and simulated streamflow are 0.82 and 0.80 in the calibration period driven
280 by gauge-based precipitation and PERSIANN-CDR precipitation, respectively. In the verification
281 period, the *NSE* values are 0.81 and 0.78 for the two types of data, respectively. The high *NSE*
282 value in both calibration and verification periods suggest that gauge-based precipitation and
283 PERSIANN-CDR precipitation have similar performances as the drivers of streamflow simulation
284 in the UYLR. In the UYZR (Figure 4 (c) and (d)), the *NSE* values are 0.63 and 0.77 in the
285 calibration period driven by gauge-based precipitation and PERSIANN-CDR precipitation
286 respectively, while they are 0.60 and 0.73 in the verification period, respectively. In both
287 calibration and verification period, the *NSE* values from PERSIANN-CDR precipitation are
288 greater than that from gauge-based precipitation, which indicates that using PERSIANN-CDR
289 precipitation as input to HIMS model is able to generate more accurate streamflow than using the
290 interpolated precipitation from a sparse gauge-network in the UYZR.

Hydrol. Earth Syst. Sci. Discuss., doi:10.5194/hess-2016-282, 2016
Manuscript under review for journal Hydrol. Earth Syst. Sci.
Published: 23 June 2016

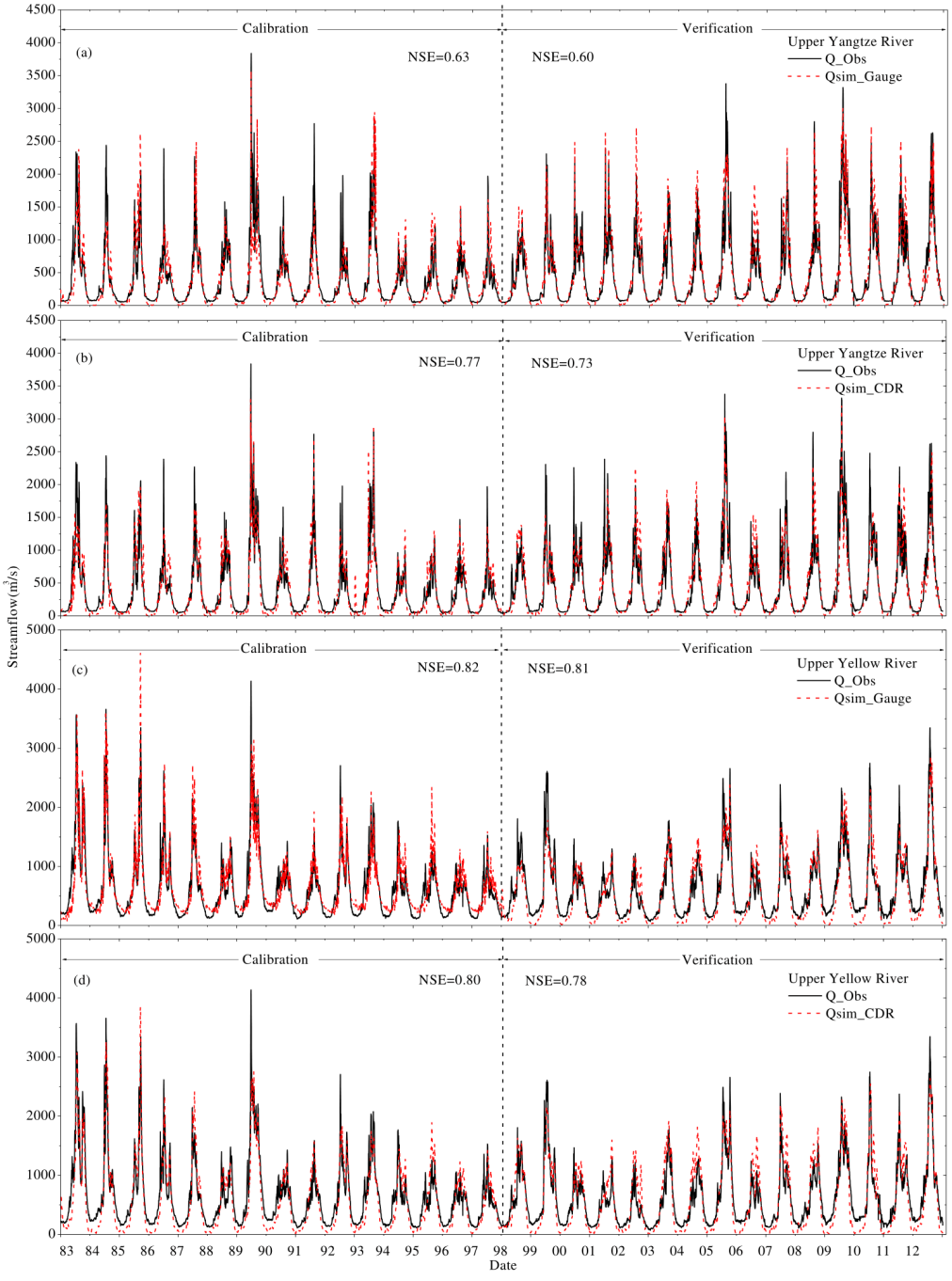

Figure 4. The comparison between the simulated daily streamflow (red) with PERSIANN-CDR

Hydrol. Earth Syst. Sci. Discuss., doi:10.5194/hess-2016-282, 2016
Manuscript under review for journal Hydrol. Earth Syst. Sci.
Published: 23 June 2016

and ground-based precipitation and the observed data (black) at the outlets of the upper Yangtze River Basin (a and b) and upper Yellow River Basin (c and d).

Table 3. Calibrated parameter values in the HIMS model for the upper Yangtze and Yellow River basins.

Basin	input	*SMSC*	*R*	*r*	L_a	R_c	*C*	K_b	C_1	C_2
Yangtze	Gauge_based	302.46	1.47	0.78	0.74	0.05	0.67	0.15	0.18	0.81
	PERSIANN-CDR	343.80	1.71	0.89	0.87	0.07	0.56	0.18	0.17	0.82
Yellow	Gauge_based	334.82	2.08	0.77	1.00	0.03	0.44	0.14	0.14	0.86
	PERSIANN-CDR	342.08	2.01	0.73	0.98	0.05	0.45	0.14	0.12	0.88

Figure 5 and Table 4 compare the simulated and observed average monthly streamflow for the two basins. In the UYZR, the relative bias between observed streamflow and simulated streamflow driven by gauge-based precipitation is 10.3% in wet season, which suggests a considerable overestimate of streamflow. Comparably, the relative bias between observed streamflow and simulated streamflow driven by PERSIANN-CDR precipitation is 0.5% in wet season. As compared with the wet season streamflow simulation results with gauge-based precipitation, the simulated streamflow driven by PERSIANN-CDR precipitation is closer to the observed streamflow. In dry season, streamflow simulations driven by gauge-based precipitation and PERSIANN-CDR precipitation both underestimate streamflow with relative bias of -22.1 and -28.0% in the UYZR, respectively. In the UYLR, both the two precipitation products slightly overestimate the streamflow in wet season with relative bias of 2.6 and 2.9%, respectively. Similar to the results in the UYZR, streamflow simulations driven by gauge-based precipitation and PERSIANN-CDR precipitation have similar good performances in wet season in the UYLR.

Hydrol. Earth Syst. Sci. Discuss., doi:10.5194/hess-2016-282, 2016
Manuscript under review for journal Hydrol. Earth Syst. Sci.
Published: 23 June 2016

However, both the two precipitation products tend to produce smaller streamflow in dry season with relative bias of -33.1% and -27.6%, respectively. One of the reasons that both PERSIANN-CDR and gauge-based precipitation generate smaller streamflow in dry season is the lack of complex method or proper algorithm in the HIMS model to handle frozen soil. In dry season, when the amounts of precipitation and streamflow are small, streamflow melted from frozen soil can account for a significant proportion of total streamflow. In other words, the frozen soil melt could significantly influence the streamflow simulation results. The relative high bias of observed streamflow and simulated streamflow from both gauge-based and satellite-based precipitation could be due to the lack of proper modeling component in the HIMS hydrologic model that quantifies the frozen soil melting effects in dry season. However, the bias between simulated and observed streamflow is much smaller in wet season, when precipitation and streamflow are relatively large and streamflow melted from frozen soil accounts for a limited proportion in total streamflow.

In summary, the streamflow simulated by PERSIANN-CDR precipitation has a good agreement with the observed streamflow in the UYZR and UYLR. The good agreement between observed streamflow and PERSIANN-CDR simulated streamflow reveals a strong streamflow simulation capability of PERSIAN-CDR product, which also gives community certain confidence in using PERSIANN-CDR product to study hydrological cycle and climate change on the Tibetan Plateau.

Hydrol. Earth Syst. Sci. Discuss., doi:10.5194/hess-2016-282, 2016
Manuscript under review for journal Hydrol. Earth Syst. Sci.
Published: 23 June 2016

Hydrology and Earth System Sciences
Discussions

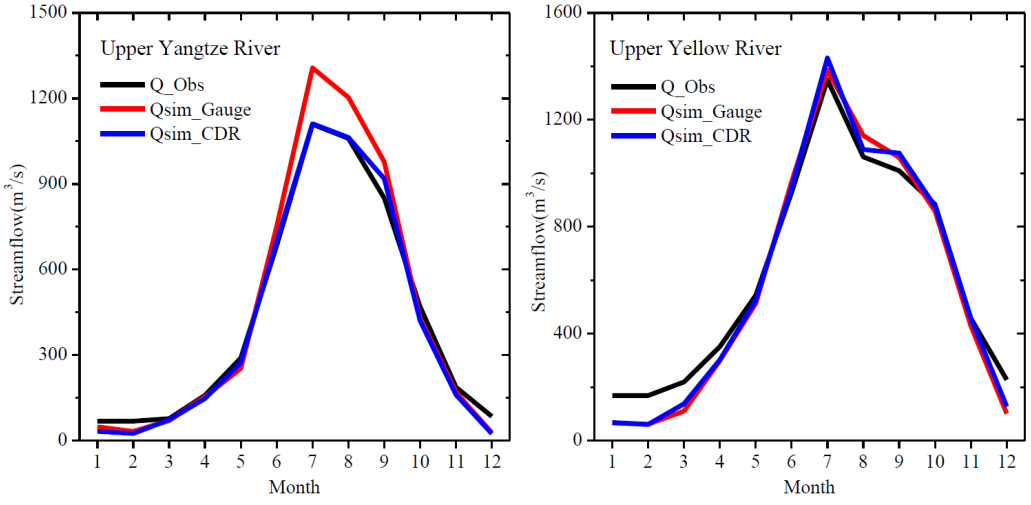

Figure 5.The comparison between the observed streamflow (black) and the simulated streamflow using PERSIANN-CDR (blue) and ground-based precipitation data (red) in the upper Yangtze River Basin and upper Yellow River Basin.

Table 4. The performances of streamflow simulations driven by gauge-based precipitation and PERSIANN-CDR precipitation in the two basins

	Upper Yangtze River					Upper Yellow River				
Period	Q_obs	Qsim_ gauge	Qsim_ CDR	Rb_ gauge	Rb _ CDR	Q_obs	Qsim_ gauge	Qsim_ CDR	Rb _ gauge	Rb _ CDR
Jan.	68.1	48.4	32.8	-28.9	-51.8	168.9	65.7	68.0	-61.1	-59.8
Feb.	68.3	32.7	24.9	-52.1	-63.5	168.3	61.6	60.5	-63.4	-64.1
Mar.	76.9	70.2	72.4	-8.7	-5.8	219.7	110.5	138.0	-49.7	-37.2
Apr.	158.6	153.2	147.5	-3.4	-7.0	352.0	299.0	302.5	-15.1	-14.0
May	289.2	253.5	273.4	-12.3	-5.5	543.6	512.9	524.9	-5.7	-3.4
Jun.	683.9	750.5	698.4	9.7	2.1	928.5	968.6	946.6	4.3	1.9
Jul.	1108.9	1306.9	1111.4	17.9	0.2	1350.1	1386.6	1431.3	2.7	6.0
Aug.	1059.7	1204.0	1063.2	13.6	0.3	1061.1	1141.4	1088.5	7.6	2.6
Sep.	850.7	977.4	918.9	14.9	8.0	1009.6	1059.7	1075.7	5.0	6.5
Oct.	469.4	428.1	420.1	-8.8	-10.5	883.7	859.1	876.5	-2.8	-0.8
Nov.	187.6	169.0	161.1	-9.9	-14.1	457.3	429.1	456.6	-6.2	-0.2
Dec.	84.5	28.2	24.5	-66.7	-71.0	227.0	100.7	127.5	-55.7	-43.9
May-Oct.	743.4	819.6	746.9	10.3	0.5	962.7	987.7	990.4	2.6	2.9
Nov.-Apr.	107.2	83.6	77.2	-22.1	-28.0	265.6	177.6	192.3	-33.1	-27.6
Annual	427.9	454.6	414.8	6.2	-3.1	617.0	586.0	594.6	-5.0	-3.6

Hydrol. Earth Syst. Sci. Discuss., doi:10.5194/hess-2016-282, 2016
Manuscript under review for journal Hydrol. Earth Syst. Sci.
Published: 23 June 2016

Hydrology and Earth System Sciences
Open Access
Discussions

Note: Q_obs indicates observed runoff (mm). Qsim_gauge and Qsim_CDR indicate streamflow simulations (mm) driven by the gauge-based precipitation and PERSIANN-CDR precipitation, respectively. Rb_gauge and Rb_CDR indicate relative bias between observed streamflow and simulated streamflow driven by the gauge-based precipitation and PERSIANN-CDR precipitation, respectively.

4. Discussions

4.1 Parameter uncertainties of hydrological modeling

In this study, model parameters are separately calibrated in terms of highest *NSE* between observed streamflow and simulated streamflow driven by gauge-based precipitation and PERSIANN-CDR precipitation. Therefore, these parameter values are highly dependent on the precipitation inputs. When the precipitation input changes, the parameter values may change accordingly in order to match the streamflow. Table 3 shows the values of calibrated parameters separately driven by gauge-based precipitation and PERSIANN-CDR precipitation in the two basins. Parameter sensitivity study of the HIMS model indicates that the HIMS model is most sensitive to parameters of the maximum soil storage capacity (*SMSC*) and the infiltration coefficients (*R* and *r*) (Jiang et al., 2015). In the UYLR, the parameters calibrated by the inputs of gauge-based precipitation and PERSIANN-CDR precipitation generally have similar values. However, in the UYZR, *SMSC*, *R* and *r* values calibrated from gauge-based precipitation are 302.46, 1.47 and 0.78 respectively, while *SMSC*, *R* and *r* values calibrated from PERSIANN-CDR precipitation are 343.80, 1.71 and 0.89 respectively. By separately calibrating the parameters in HIMS model, gauge-based precipitation and PERSIANN-CDR result in different optimal parameter values. . Thus, the streamflow simulation bias using gauge-based precipitation and PERSIANN-CDR are the joint results of parameter differences and model input bias. Correspondingly, soil moisture and evapotranspiration estimation could be different using various

Hydrol. Earth Syst. Sci. Discuss., doi:10.5194/hess-2016-282, 2016
Manuscript under review for journal Hydrol. Earth Syst. Sci.
Published: 23 June 2016

363 precipitation forcings and calibrated parameters. However, the main purpose of this study is
364 evaluating the streamflow simulation capability of satellite-based precipitation and gauge-based
365 precipitation as inputs to a hydrologic model over the Tibetan Plateau. Therefore, in spite of the
366 influence of cancellation between parameter differences and precipitation bias on streamflow
367 simulation, it does not harm the conclusion that PERSIANN-CDR precipitation is able to produce
368 a reasonably good streamflow in the two river basins on the Tibetan Plateau.

369 In previous study, Tong et al. (2014) evaluated the streamflow simulation capabilities of four
370 satellite-based precipitation products (TRMM-3B42-V7, TRMM-3B42RT-V7, PERSIANN and
371 CMORPH) using the VIC hydrologic model in the UYZR and UYLR from 2006 to 2012. Different
372 from the PERSIANN product that Tong et al. (2014) used, PERSIANN-CDR is a different product
373 that provides over 33 years of daily and high resolution precipitation with GPCP monthly
374 information incorporated. In addition, the parameters in the VIC hydrologic model are calibrated
375 by the input of interpolated gauge-based precipitation. The calibrated parameter values are then
376 kept fixed when the VIC model are rerun by inputs of satellite-based precipitation datasets to
377 evaluate the streamflow simulation capabilities of satellite-based precipitation datasets. Rerunning
378 the hydrologic model with the fixed parameters calibrated by gauge-based precipitation partly
379 indicates that the authors consider the sparse gauge observations a more reliable dataset than
380 satellite-based precipitation datasets. However, this is a questionable assumption. As we mentioned
381 in the introduction, not only because the location of rain-gauges is conditioned (relatively low
382 elevations), but also the sparse distribution of rainfall stations over the Tibetan Plateau could bring
383 large errors and uncertainties in regional rainfall measurement. We rather cautiously believe that
384 gauge-based precipitation could not be reliable, especially in the UYZR where there is only one
385 station per 34426 km^2 (nearly $1^\circ \times 3^\circ$ spatial resolution). Therefore, separately calibrating

Hydrol. Earth Syst. Sci. Discuss., doi:10.5194/hess-2016-282, 2016
Manuscript under review for journal Hydrol. Earth Syst. Sci.
Published: 23 June 2016

hydrologic model by the inputs of different precipitation datasets instead of using identical parameters will contribute to fairer comparisons when evaluating streamflow simulation capabilities of different precipitation datasets, though other hydrological variables such as soil moisture and evapotranspiration could be incorrectly estimated by different precipitation inputs and calibrated parameters.

4.2 The influences of precipitation record length on streamflow simulation capability

Besides of the uncertainties due to hydrological model calibration, another factor that influences the accuracy of streamflow simulation is the length of precipitation records used for calibration. As mentioned before, one of the advantages of PERSIANN-CDR product is the provision of more than 33 years of continuous sequences of precipitation data, which can allow more extensive streamflow simulation in the Tibetan Plateau. In this study, comparison experiments (Figure 6) were designed to test the influences of precipitation record length on the accuracy of streamflow simulation. In the experiments, we investigate the accuracy of streamflow simulation during 2008 to 2012 with two different calibration scenarios. In the first scenario, the calibration period is from 2003 to 2007 for both the UYZR (Figure 6a) and the UYLR (Figure 6b). In the second scenario (Figure 6c and 6d), 15 years of data from 1983 to 1997 is used for calibration, which is longer than that in the first scenario. As it is shown in Figure 6 (a and b), in the first scenario the *NSE* values between daily observed and simulated streamflow are 0.75 and 0.66 during the verification period (from 2008 to 2012) for the UYZR and UYLR, respectively. Comparatively, in the second scenario the *NSE* values during the verification period (from 2008 to 2012) are 0.81 and 0.82 for the two basins, respectively. The *NSE* values in the second scenario are consistently higher than that in the first scenario in the two basins. For the UYLR in the second scenario (Figure 6d), the *NSE* value during the verification period is significantly greater than that

Hydrol. Earth Syst. Sci. Discuss., doi:10.5194/hess-2016-282, 2016
Manuscript under review for journal Hydrol. Earth Syst. Sci.
Published: 23 June 2016

409 in the first scenario. Figure 6(b) also shows that the HIMS hydrological model significantly
410 underestimates the flow peaks during the summer of 2010 and 2012 when calibrated by 5 years of
411 data from 2003 to 2007. The disagreement between the observed and simulated flow peaks is partly
412 because the magnitudes of flood events during the calibration period are all smaller than that during
413 the verification period and the HIMS hydrological model cannot be well trained during the
414 calibration period. Therefore, when using a short length precipitation data as input for a
415 hydrological model, the accuracy of streamflow simulation could be limited, especially when
416 precipitation data used for calibration cannot cover the flood and drought conditions of a basin.
417 However, when the HIMS hydrological model is calibrated by the longer dataset from 1983 to
418 1997 as it is shown in Figures 6c and d, there is a greater potential that the characteristics of
419 extreme events can be captured by the hydrological model than only using 5 years of data from
420 2003 to 2007. Given the availability of long-term precipitation records (over 33 years) provided
421 by PERSIANN-CDR product, the extreme events in the historical period could be well captured
422 by a hydrological model. Therefore, using such a product with long-term records, the confidence
423 of simulating streamflow over the Tibetan Plateau will correspondingly increase.

Hydrol. Earth Syst. Sci. Discuss., doi:10.5194/hess-2016-282, 2016
Manuscript under review for journal Hydrol. Earth Syst. Sci.
Published: 23 June 2016

Hydrology and Earth System Sciences
Discussions

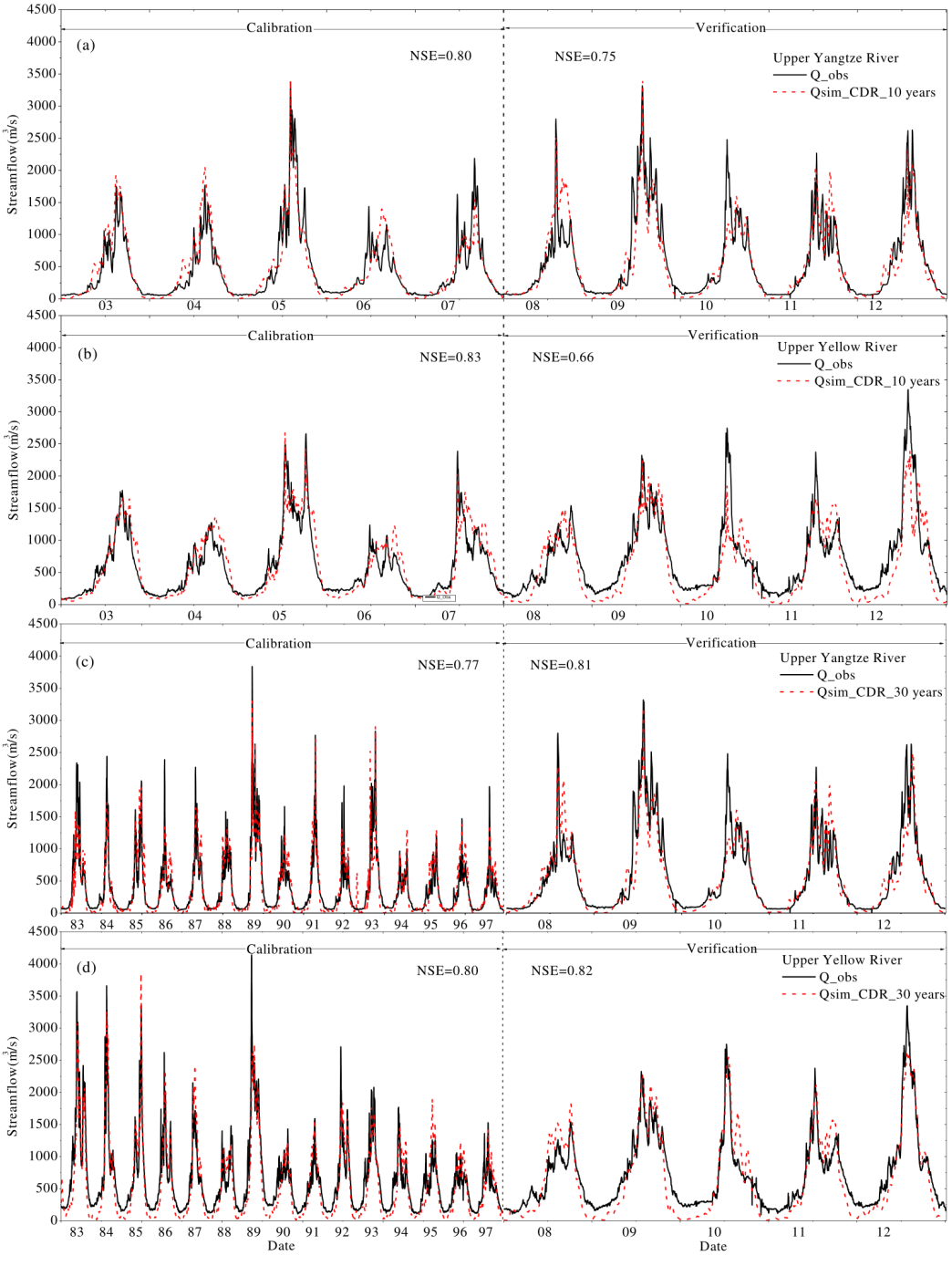

Figure 6. The simulated daily streamflow (red) forced by PERSIANN-CDR rainfall product in

Hydrol. Earth Syst. Sci. Discuss., doi:10.5194/hess-2016-282, 2016
Manuscript under review for journal Hydrol. Earth Syst. Sci.
Published: 23 June 2016

426 different scenarios and the observed daily streamflow (black) at the outlets of the upper Yangtze
427 River Basin and upper Yellow River Basin. (a) and (b) is the scenario that the period 2003 to 2007
428 is used for calibration and 2008 to 2012 for verification. (c) and (d) is the scenario that the period
429 1983 to 1997 is used for calibration and 2008 to 2012 for verification
430

431 5. Summary

432 As it is compared to radar-based precipitation measurement and gauge networks, the main
433 advantage of satellite-based precipitation estimate is the broader coverage at global scale. This
434 allows a comprehensive understanding of the driving force of hydrologic cycle, especially for the
435 gauge sparse area. To verify the accuracy of satellite-based precipitation estimate products, the
436 comparison with ground observation is necessary. However, in gauge sparse area, a direct
437 comparison on precipitation temporal and spatial variation will be arguable due to the limited
438 gauge information. This study provides an alternative way to evaluate satellite-based precipitation
439 products by forcing both rainfall estimates from satellite and limited gauge network into
440 hydrological model. Given the confidence in streamflow measurements, which are more reliable
441 and well monitored than the limited ground-based rainfall measurements, the comparison of
442 simulated streamflow enables an indirect way to evaluate satellite-based precipitation products.
443 In this study, PERSIANN-CDR precipitation and gauge-based precipitation have good
444 agreements in the UYLR, while the two datasets have different values in the UYZR. Streamflow
445 simulation capabilities of PERSIANN-CDR precipitation and gauge-based precipitation are
446 evaluated as the inputs of the HIMS hydrologic model in the two basins. Both the two datasets
447 have similar good performances in the UYLR, while PERSIANN-CDR precipitation has slightly
448 better performance than gauge-based precipitation in the UYZR. Gauge-based precipitation tends

Hydrol. Earth Syst. Sci. Discuss., doi:10.5194/hess-2016-282, 2016
Manuscript under review for journal Hydrol. Earth Syst. Sci.
Published: 23 June 2016

449 to produce larger streamflow in wet season in the UYZR. This indicates that in the UYZR, a sparse
450 gauge network are not a completely reliable reference for water resources management and
451 operation due to the fact that the locations of the limited gauge stations cannot be representative
452 for measuring the precipitation patterns at the river basin scale.

453 Lack of rainfall gauge stations has brought great challenge to hydrological and climate studies
454 over the Tibetan Plateau (e.g., Yao et al., 2012; Zhang et al., 2013). Based on the demonstration in
455 this study that PERSIANN-CDR is able to produce reasonably good streamflow in the UYZR and
456 UYLR as compared to observed streamflow, we can speculated that PERSIANN-CDR rainfall
457 product has the potential to be a useful dataset and alternative of the sparse gauge network for
458 future climate change and hydrological studies on the Tibetan Plateau considering the needs for
459 long-term (more than 33 years) and high resolution records.

460

461 **Data Availability**

462 The PERSIANN-CDR data used in this study is available from the NOAA CDR Program
463 (https://www.ncdc.noaa.gov/cdr/atmospheric/precipitation-persiann-cdr) and gauge data is
464 retrieved from China Meteorological Administration database (http://www.cma.gov.cn/en2014/
465 and http://data.cma.cn/). The data is public accessible by user registration from the providing
466 agencies.

467

468 **Acknowledgements**

469 This research was supported by the Natural Science Foundation of China (41571024, 41330529,
470 41201034), the program for "Bingwei" Excellent Talents in Institute of Geographic Sciences and
471 Natural Resources Research, CAS (Project No.2013RC202) and the NOAA NCDC/Climate Data

Record program (Prime Award NA09NES440006).

Reference

Adler, R.F., Huffman, G.J., Chang, A., Ferraro, R., Xie, P., Janowiak, J., Rudolf, B., Schneider, U., Curtis, S., Bolvin, D., Gruber, A., Susskind, J., Arkin, P., Nelkin, E., 2003. The version-2 global precipitation climatology project (GPCP) monthly precipitation analysis (1979-present). *J. Hydrometeorol.* 4, 1147 – 1167.

Ashouri, H., and Coauthors, 2015: PERSIANN-CDR: Daily precipitation climate data record from multisatellite observations for hydrological and climate studies. *Bull. Amer. Meteor. Soc.*, 96, 69–83, doi:10.1175/BAMS-D-13-00068.1.

Artan, G., Gadain, H., Smith, J.L., Bandaragoda, C.J., Verdin, J.P., 2007. Adequacy of satellite derived rainfall data for stream flow modeling. *Nat. Hazards* 43 (2),167 – 185.

Bitew, M.M., Gebremichael, M., Ghebremichael, L.T., Bayissa, Y.A., 2012. Evaluation of high-resolution satellite rainfall products through streamflow simulation in a hydrological modeling of a small mountainous watershed in Ethiopia. *J. Hydrometeorol.* 13 (1), 338–350.

Casse, C., Gosset, M., Vischel, T., Quantin, G. and Tanimoun, B. (2015) Model-based study of the role of rainfall and land use land cover in the changes in Niger Red floods occurrence and intensity in Niamey between 1953 and 2012. Hydrology and Earth System Sciences Discussions 12, 12039-12087.

Duan, Q., Sorooshian, S., & Gupta, V. (1992). Effective and efficient global optimization for conceptual rainfall-runoff models. *Water Resour. Res*, 28(4), 1015-1031.

Franchini, M., Lamberti, P., 1994. A flood routing Muskingum type simulation and forecasting model based on level data alone,. Water Resour. Res. 30 (7), 2183e2196.

495 Garcia, M., Peters-Lidard, C.D., Goodrich, D.C., 2008. Spatial interpolation of precipitation in a
496 dense gauge network for monsoon storm events in the southwestern United States. *Water*
497 *Resour. Res*. 44, W05S13, http://dx.doi.org/10.1029/2006WR005788.
498 Hargreaves, G.H. and Samani, Z.A., 1985. Reference crop evapotranspiration from temperature.
499 *Appl. Eng. Agric.* 1 (1), 96-99.
500 Huffman, G. J., and Coauthors, 1997: The Global Precipitation Climatology Project
501 (GPCP)combined precipitation dataset. *Bull.Amer. Meteor. Soc.*, 78, 5–20, doi:10.1175/1520-
502 0477(1997)078,0005:TGPCPG.2.0.CO;2.
503 Hock, R. (2003), Temperature index melt modelling in mountain areas, *J. Hydrol.*, 282(1–4), 104–
504 115, doi:10.1016/S0022-1694(03)00257-9.
505 Liu, C.M., Zheng, H.X., Wang, Z.G., et al., 2006. Distributed Simulation of Catchment Water
506 Cycle. Yellow River Conservancy Press, Zhengzhou, China.
507 Liu, C.M., Wang, Z.G., Zheng, H.X., Zhang, L., Wu, X.F., 2008. Development and application of
508 HIMS system. Sci. China (E) 38 (3), 350e360.
509 Liu, C.M.,Wang, Z.G., Yang, S.T., Zheng, H.X., 2010a. Research progress of water cycle
510 integrated simulation system (HIMS). Water Resour. Dev. Res. 8 (3), 5e15 (in Chinese).
511 Liu, C.M., Zheng, H.X., Wang, Z.G., Yang, S.T., 2010b. Multi-Scale integrated simulation of
512 hydrological processes using HIMS with verified case studies. J. Beijing Norm. Univ. Nat.
513 Sci. 46 (3), 268e273 (in Chinese).
514 Ly, S., Charles, C., Degre, A., 2011. Geostatistical interpolation of daily rainfall at catchment scale:
515 the use of several variogram models in the Ourthe and Ambleve catchments, Belgium. Hydrol.
516 Earth Syst. Sci. 15, 2259 – 2274.
517 Joyce, R.J., Janowiak, J.E., Arkin, P.A., Xie, P., 2004. CMORPH: a method that produces global

precipitation estimates from passive microwave and infrared data at high spatial and temporal resolution. J. Hydrometeorol. 5 (3), 487 – 503

Kidd, C. and Levizzani, V., 2011. Status of satellite precipitation retrievals. *Hydrol. Earth Syst. Sci.* 15, 1109 – 1116.

Miao, C., H. Ashouri, K.-L. Hsu, S. Sorooshian, and Q. Duan, 2015, Evaluation of the PERSIANN-CDR daily rainfall estimates in capturing the behavior of extreme precipitation events over China, *J. Hydrometeorol.*, doi:10.1175/JHM-D-14-0174.1.

Nalder, I.A., Wein, R.W., 1998. Spatial interpolation of climatic normals: test of a new method in the Canadian boreal forest. Agr. For. Meteorol. 92 (4), 211 – 225.

Sheffield, J., et al. (2014), A drought monitoring and forecasting system for sub-Sahara African water resources and food security, *Bull. Amer. Meteor. Soc.*, 95, 861-882, doi: 10.1175/BAMS-D-12-00124.1.

Su, F., Gao, H., Huffman, G.J., Lettenmaier, D.P., 2011. Potential utility of the realtime TMPA-RT precipitation estimates in Streamflow prediction. *J.Hydrometeorol*. 12, 444 – 455.

Sorooshian, S., Hsu, K.-L., Gao, X., Gupta, H.V., Imam, B., Braithwaite, D., 2000. Evaluation of PERSIANN system satellite-based estimates of tropical rainfall. *Bull. Am. Meteorol. Soc.* 81 (9), 2035 – 2046.

Sorooshian, S., and Coauthors, 2011: Advancing the remote sensing of precipitation. *Bull. Amer. Meteor. Soc.*, 92, 1271–1272, doi:10.1175/BAMS-D-11-00116.1.

Thom, H. C. S. (1958), A note on the gamma distribution, Mon. Wea. Rev., 86, 117-122, doi:10.1175/1520-0493(1958)086<0117:ANOTGD>2.0.CO;2.

Tong, K., F. Su, D. Yang, and Z. Hao, 2014: Evaluation of satellite precipitation retrievals and their potential utilities in hydrologic modeling over the Tibetan Plateau. *J. Hydrol.*, 519, 423–

437, doi:10.1016/j.jhydrol.2014.07.044.

Turk, F.J., Miller, S.D., 2005. Toward improved characterization of remotely sensed precipitation regimes with MODIS/AMSR-E blended data techniques. *IEEE Trans. Geosci. Rem. Sens.* 43 (5), 1059 – 1069.

Xie, P. P., J. E. Janowiak, P. A. Arkin, R. Adler, A. Gruber, R. Ferraro, G. J. Huffman, and S. Curtis, 2003: GPCP Pentad precipitation analyses:An experimental dataset based on gauge observations and satellite estimates. *J. Climate*, 16, 2197–2214, doi:10.1175/2769.1.

Yilmaz, K.K., Hogue, T.S., Hsu, K.-L., Sorooshian, S., 2005. Intercomparison of rain gauge, radar, and satellite-based precipitation estimates with emphasis on hydrologic forecasting. *J. Hydrometeorol.* 6 (4), 497 – 517.

Yong, B., Ren, L., Hong, Y., Wang, J., Gourley, J., Jiang, S., Chen, X., Wang, W., 2012. Assessment of evolving TRMM-based multisatellite real-time precipitation estimation methods and their impacts on hydrologic prediction in a high latitude basin. *J. Geophys. Res.* 117, D09108, http://dx.doi.org/ 10.1029/2011JD017069.

Yao, T. D., et al. (2012), Different glacier status with atmospheric circulations in Tibetan Plateau and surroundings, Nat. Clim. Change, 2(9), 663–667.

Zhang, L., Su, F., Yang, D., Hao, Z. and Tong, K. (2013). Discharge regime and simulation for the upstream of major rivers over Tibetan Plateau. *J. Geophys. Res.*, 118, http://dx.doi.org/10.1002/jgrd.50665.

Zhang X. and Tang Q (2015). Combining satellite precipitation and long‐term ground observations for hydrological monitoring in China. *J. Geophys. Res.*, doi: 10.1002/2015JD023400

Zhang, Y., S. Liu, and Y. Ding (2006), Observed degree-day factors and their spatial variation on

Hydrol. Earth Syst. Sci. Discuss., doi:10.5194/hess-2016-282, 2016
Manuscript under review for journal Hydrol. Earth Syst. Sci.
Published: 23 June 2016

564 glaciers in western China, *Ann. Glaciol.*, 43(1), 301–306

565

566

567 **Figure Captain**

568 Figure 1. The selected river basins (the upper Yellow River and Yangtze River Basin) on the
569 Tibetan Plateau and location of rainfall stations and river outlets.

570 Figure 2. The monthly average runoff observed at the river outlet of the upper Yangtze River and
571 Yellow River Basin, and the precipitation data retrieved from PERSIANN-CDR and ground-based
572 observation.

573 Figure 3. The calculated CDF of rainfall from PERSIANN-CDR and ground-based observation in
574 the upper Yangtze River Basin and upper Yellow River Basin.

575 Figure 4. The comparison between the simulated daily streamflow (red) with PERSIANN-CDR
576 and ground-based precipitation and the observed data (black) at the outlets of the upper Yangtze
577 River Basin (a and b) and upper Yellow River Basin (c and d).

578 Figure 5.The comparison between the observed streamflow (black) and the simulated streamflow
579 using PERSIANN-CDR (blue) and ground-based precipitation data (red) in the upper Yangtze
580 River Basin and upper Yellow River Basin.

581 Figure 6. The simulated daily streamflow (red) forced by PERSIANN-CDR rainfall product in
582 different scenarios and the observed daily streamflow (black) at the outlets of the upper Yangtze
583 River Basin and upper Yellow River Basin. (a) and (b) is the scenario that the period 2003 to 2007
584 is used for calibration and 2008 to 2012 for verification. (c) and (d) is the scenario that the period
585 1983 to 1997 is used for calibration and 2008 to 2012 for verification